HHS Public Access

Author manuscript

*Nature*. Author manuscript; available in PMC 2014 April 10.

Published in final edited form as:

*Nature*. 2013 March 14; 495(7440): 241–245. doi:10.1038/nature11979.

# Ovarian surface epithelium at the junction area contains cancer-prone stem cell niche

**Andrea Flesken-Nikitin**[1], **Chang-Il Hwang**[1], **Chieh-Yang Cheng**[1], **Tatyana V. Michurina**[2,3], **Grigori Enikolopov**[2,3], and **Alexander Yu. Nikitin**[1,*]

[1]Department of Biomedical Sciences and Cornell Stem Cell Program, Cornell University, Ithaca, New York 14853, USA

[2]Cold Spring Harbor Laboratory, Cold Spring Harbor, NY 11724, USA

[3]NBIK, Moscow Institute of Physics and Technology, Dolgoprudny 141700, Russia

## Abstract

Epithelial ovarian cancer (EOC) is the fifth-leading cause of cancer death among women in the United States, but its pathogenesis is poorly understood [1-3]. Some epithelial cancers are known to occur in transitional zones between two types of epithelium, while others have been shown to originate in epithelial tissue stem cells [4-6]. The stem cell niche of the ovarian surface epithelium (OSE), which is ruptured and regenerates during ovulation, has not yet been unequivocally defined. Here we identify the hilum region of the mouse ovary, the transitional/junction area between OSE, mesothelium and tubal (oviductal) epithelium as a previously unrecognized stem cell niche of the OSE. We find that cells of the hilum OSE are slowly-cycling and express stem/progenitor cell markers ALDH1, Lgr5, Lef1, CD133, and CK6b. These cells display long-term stem cell properties ex vivo and in vivo, as shown by our serial sphere generation and by long-term lineage tracing assays. Importantly, the hilum cells exhibit increased transformation potential after inactivation of tumour suppressor genes *Trp53* and *Rb1*, whose pathways are frequently altered in the most aggressive and common type of human EOC, high-grade serous adenocarcinoma [7,8]. Our study experimentally supports the notion that susceptibility of transitional zones to malignant transformation may be explained by the presence of stem cell niches in those areas. Identification of a stem cell niche for the OSE may have important implications for understanding EOC pathogenesis.



*Correspondence: Alexander Yu. Nikitin, Department of Biomedical Sciences, Cornell University, T2014 VRT Campus Rd., Ithaca, NY, 14853. an58@cornell.edu.

**Author Contributions** A.F.N. and A.Y.N. designed the study, interpreted data and wrote the manuscript. A.F.N., C.I.H., C.Y.C., T.V.M. and G.E. performed experiments and analyzed data. All authors discussed the results and commented on the manuscript.

**Author Information** Microarray data discussed in this publication have been deposited in NCBI's Gene Expression Omnibus and are accessible through GEO Series accession number GSE43897. Reprints and permissions information is available at www.nature.com/reprints. The authors declare no competing financial interests. Correspondence and requests for materials should be addressed to A.Y.N. (an58@cornell.edu).

Supplementary Information is linked to the online version of the paper at www.nature.com/nature

**Keywords**

ovarian carcinoma; stem cell compartment; regeneration

An extensive integrated genomic analysis of 489 high-grade serous ovarian adenocarcinomas has provided important insights about repertoire of molecular aberrations characteristic for this most common and deadly form of EOC [7]. However, interpretation of such results is complicated by continuous controversy about the cell of origin of this disease. The OSE, the fimbrial epithelium of the uterine (Fallopian) tubes, and other derivatives of the secondary Mullerian system have been proposed as likely sources of EOC based on pathological observations, genetic and immunohistochemical studies of precursor lesions in human cancer and experimental approaches in several species [2,3,9,10]. Recently, it has been hypothesized that transitional/junction regions between the OSE, mesothelium, and tubal epithelium may have more plastic and, presumably, less differentiated state, thereby being a possible place of origin of EOC [5,11,12]. However, to date there are no direct experimental data to support this notion.

Stem cells, such as those of blood and hair, are slow-cycling and retain DNA label in pulse-chase experiments. Few years ago, OSE cells with some stem/progenitor cell properties have been identified based on their slow proliferation in label retention assays [13]. Unfortunately, it remains uncertain if these cells have potential for long-term self-renewal, a key feature of stem cells. It is also unknown if these cells occupy anatomically defined areas, similar to those in other organs, such as the intestine, hair follicle, cornea and prostate [14,15]. Activity of detoxifying enzyme aldehyde dehydrogenase (ALDH) and corresponding expression of ALDH1 have been identified as a useful marker of stem/progenitor cells in a number of cell lineages, such as mammary, prostate, colon, hematopoietic, neural, and mesenchymal [16-19]. It has been also reported that about 7.6 % of OSE cells have high ALDH activity [20]. Thus we tested if detection of this activity can be used for enrichment of normal OSE stem/progenitor cells. We separated primary OSE cells into ALDH high ($ALDH^+$) and ALDH low ($ALDH^-$) populations according to their level of ALDEFLUOR fluorescence by fluorescence activated cell sorting (FACS, Supplementary Fig. 1), and subjected them to newly established monoclonal OSE-sphere formation assays (Fig. 1a, b and Supplementary Fig. 2, 3). $ALDH^+$ cells represented 5.3% of OSE population and formed larger OSE spheres and at significantly higher frequency as compared to $ALDH^-$cells (Supplementary Fig. 4 and Supplementary Table 1). Consistent with expected self-renewal properties of stem/progenitor cells, spheres were formed from a single cell suspension in at least 5 consecutive rounds of sphere dissociation and regeneration (Fig. 1c).

Towards identification of $ALDH1^+$ OSE cells in the mouse ovary we have performed immunohistochemical staining for ALDH1 expression in ovarian tissues from 3, 6 and 8 weeks old virgin FVB/N, C57BL/6J, B6;129 and Swiss Webster mice. Since the ovary has well defined anatomical regions, we have evaluated expression of ALDH1 in the OSE covering the corpus luteum, the distal, antral and the hilum regions, as well as in the tubal epithelium. Strikingly, in mice of all age and strain groups, cells with high ALDH1 activity have been predominantly detected in the hilum region (Fig. 1d and Supplementary Fig. 5).

This region represents the point where nerves and vessels enter the ovary and is covered by the epithelium representing the transition between OSE, mesothelium and tubal epithelium.

To determine the location of slow proliferating cells we performed pulse-chase experiments by injecting 6 - 7 weeks old virgin FVB/N mice for 10 days with a BrdU solution followed by detection of label retaining cells (LRCs) immediately and monthly for up to 3 months after the pulse (Supplementary Fig. 6a). Ovarian regional analysis revealed that the hilum contains the highest percent of slow-cycling OSE cells by 3 months after BrdU pulse (Fig. 1e and Supplementary Fig. 6b). These LRCs expressed ALDH1, as shown by double immunofluorescence (Fig. 1f). In agreement with earlier reports [13,21], proliferation of OSE was significantly greater after ovulation. To test if LRCs preferentially divide after ovulation, cells double positive for BrdU and Ki67 were scored in the hilum areas of mice subjected to 2 and 3 months BrdU pulse chase experiments and sacrificed either in proestrus (prior to ovulation) or estrus (after ovulation). Double positive cells were present in the hilum OSE of mice only in estrus, no such cell were found in proestrus (Supplementary Fig. 7), suggesting that these LRCs were activated to repair the ruptured OSE.

We assessed the growth potential of OSE cells isolated by micro-dissection from the hilum (posterior) and opposite part (anterior) regions of the ovary (Supplementary Fig. 8). After three days of primary culture hilum OSE cells formed significantly more large colonies (over ≥ 20 cells) than OSE from the anterior region (Fig. 2a, b). Notably, hilum cells developed spheres at significantly higher frequency as compared to other OSE cells, which could be propagated for at least 7 generations (Fig. 2c, Supplementary Fig. 9 and Supplementary Table 2). These findings are consistent with results of our previous experiments with $ALDH^+$ cells.

For additional phenotypical characterization $ALDH^+$ and $ALDH^-$ OSE cells were isolated by FACS and their RNA used for gene expression profiling (Fig. 2d, Supplementary Fig. 10 and Supplementary Table 3). *Aldh1* gene was among the highest expressed genes in $ALDH^+$ cells (Supplementary Fig. 10). Among known stem cell markers Lgr5, CD133, CK6b, and Lef1 were consistently higher in $ALDH^+$ cells (Fig. 2e). Expression of these markers in the hilum cells was also confirmed by immunostaining (Fig. 2f). Consistently, we have found that some of microRNAs counteracting stem cell properties, such as microRNAs of miR-34 family [22-24] as well as miR-376b (our unpublished data), are preferentially downregulated in $ALDH^+$ OSE cells relative to the $ALDH^-$ OSE population (Fig. 2g).

Since hilum cells express Lgr5, for tracing the fate of these cells we have taken an advantage of *Lgr5*$^{tm1(cre/ERT2)Cle}$/J (Lgr5-EGFP-IRES-creERT2) mice, which harbor a Lgr5-EGFP-IRES-CreERT2 “knock-in” allele [25]. In these mice, EGFP and Cre-ERT2 are expressed in Lgr5 positive cells. However, activity of Cre-ERT2 fusion protein occurs only after induction by tamoxifen. We have crossed Lgr5-EGFP-IRES-creERT2 mice with *Gt(ROSA)26Sor*$^{tm9(CAG-tdTomato)Hze}$/J (Ai9) mice (Supplementary Fig. 11). In Ai9 mice expression of Rosa26/CAG promoter-driven red fluorescent protein variant (tdTomato) is possible only after Cre-mediated deletion of the *STOP* codon flanked by *loxP* sites [26]. To test if *Lgr5* promoter directs Cre expression to the hilum cells, mice were exposed to a single dose of tamoxifen and their ovaries have been collected 1 and 3 days later. Microscopy

analysis showed that cells of the hilum have been exclusively labeled in the OSE at these early time points (Fig. 3a-c and Supplementary Fig. 12a-g). Control experiments included administration of oil to double knock-in littermates (Fig. 3d, e and Supplementary Fig. 12h-j). Also wild-type mice and mice carrying only one of the knock-in alleles have been analyzed with and without tamoxifen administration. To test if Lgr5-expressing hilum cells contribute to the rest of the OSE, we collected ovaries of Lgr5-EGFP-IRES-creERT2 Ai9 mice at 1 and 2 months after tamoxifen administration. The majority of OSE cells in tamoxifen but not control experiments expressed tdTomato, indicating that the hilum cells contribute to regeneration of the OSE covering the ovary (Fig. 3f and Supplementary Fig. 12k, l).

*TP53* mutations and alterations of RB1 pathway occur in 96% and 67%, respectively, of human high-grade serous adenocarcinomas [7,8], and result in formation of similar malignancies in genetically modified mice [27,28]. Thus we have compared proliferation and immortalization efficiency of the OSE cells located at the hilum and in the remainder of the ovary after conditional inactivation of *Trp53* and *Rb1* (Supplementary Fig. 13). The hilum cells have exhibited significantly increased proliferation and were passaged for over 20 times without crisis phase. At the same time the majority of the remainder OSE cell pool have become senescent by passage 6 according to their enlarged flattened shape and expression of senescence markers, such as of senescence-associated β galactosidase, p16 and p27 (Fig. 4a-c and Supplementary Fig. 14).

We have also carefully evaluated various regions of the ovary for the early stages of carcinogenesis induced by Cre-*LoxP* mediated recombination after a single administration of AdCre into the ovarian bursa. Such administration results in infection of over 80% of cells in all anatomical regions of the ovary followed by formation of *Trp53* and *Rb1*-deficient neoplastic lesions in a relatively synchronous manner (Supplementary Fig. 15, 16 and [27]) The earliest atypical cells were detected in the hilum and adjacent areas but not in the other regions of the ovary or in the tubal epithelium in 12 of 16 mice (75%) by 60 days after induction (Supplementary Fig. 17 and Supplementary Table 4).

To directly test tumourigenic properties of *Trp53* and *Rb1*-deficient primary OSE cells we transplanted them intraperitoneally (i.p.) and subcutaneously (s.c.). In i.p. experiments, seven out of eight mice (87%) transplanted with the hilum cells developed high-grade serous adenocarcinomas characterized by extensive proliferation and expression of cytokeratin 8 (CK8), Wilms Tumour 1 (WT1), PAX8, Estrogen Receptor α (ER), Ephrin B1 and ALDH1 (Fig. 4d-n and Supplementary Fig. 18, 19). Notably, 5 of 7 neoplasms (71%) metastasized to the lung (Fig 4l-n and Supplementary Fig. 18d-f). Only one out of 12 mice (8%) transplanted with the remainder OSE cells developed carcinoma. This neoplasm expressed CK8, WT1, ER, but contained less of ALDH1 highly-positive cells, only few PAX8 positive cells, and was not metastatic (Supplementary Fig. 19, 20). Similar results were also observed in s.c. experiments (Supplementary Fig. 19-21 and Supplementary Table 5). Thus, the hilum cells have increased transformation potential after inactivation of *Trp53* and *Rb1* and may be the cell of origin of EOC.

In summary, we show that the OSE at junction areas contains a novel stem cell niche, which is responsible for OSE regeneration and is prone to malignant transformation. These findings provide experimental rationale for targeted detection and characterization of preneoplastic and early neoplastic lesions in the areas of transition between OSE, mesothelium and tubal epithelium in humans. Presence of adult stem cells in the areas of a junction between two types of epithelia has been definitively demonstrated only for the limbus region, a narrow transitional zone between the cornea and bulbar conjunctiva [29] and gastroesophageal junction [30]. However, it remains insufficiently elucidated if such junction-associated stem cell niches are predisposed to cancer. Our findings support this possibility and suggest that similar junction areas in other organs, such as the uterine cervix and the anus, may also contain cancer-prone stem cell niches, thereby explaining susceptibility of such regions to malignant transformation. Given the well anatomically defined location of the hilum in the mouse ovary, this region may represent an attractive model for further studies aimed to understand why stem cell niches reside in the junction areas and how aberrations in the molecular and cellular mechanisms governing epithelium regeneration may contribute to ovarian carcinoma pathogenesis.

## Methods

### Experimental animals

FVB/NCr (FVB/N) and Swiss Webster (Cr:SW) mice were purchased from NCI-Frederick Animal Production Program (Charles River Laboratories, Frederick, MD) or bred in house. C57BL/6J (B6) mice and B6;129 crosses were bred in house. The β-actin EGFP (C57BL/6-Tg(CAG-EGFP01Osb/J), β-actin DsRed [B6.Cg-Tg(ACTB-DsRed*MST)1Nagy/J], *Lgr5*$^{tm1(cre/ERT2)Cle}$/J (Lgr5-EGFP-IRES-creERT2), *Gt(ROSA)26Sor*$^{tm9(CAG-tdTomato)Hze}$/J (Ai9) and NOD.Cg-*Prkdc*$^{scid}$*Il2rg*$^{tm1Wjl}$/SzJ mice were purchased from The Jackson Laboratory (Bar Harbor, ME). *Trp53*$^{loxP/loxP}$ and *Rb1*$^{loxP/loxP}$ mice were received from Dr. Anton Berns (The Netherlands Cancer Institute, Amsterdam, Netherlands). All mice were maintained identically, following recommendations of the Institutional Laboratory Animal Use and Care Committee.

### Isolation of primary OSE cells

Individual ovaries were dissected from 6 to 8 weeks old virgin FVB/N or wild type mice, transferred to 100 μl digestion-buffer (D-Buffer, 4 mg Collagenase-Dispase (Roche, Indianapolis, IN) /ml DMEM/F12 (Ham's) medium (Mediatech, Manassas, VA) supplemented with 30 mg/ml bovine albumin (Sigma, St. Louis, MO) and 1 μl Deoxyribonuclease I, (DNaseI; 1 mg/ml, Sigma), incubated for 55 minutes at 37°C in a 5% CO2 incubator. After the incubation, ovaries were removed, 5 ml complete OSE Stem Cell Medium (OSE-SCM, DMEM/F12 (Ham's) medium (Mediatech) containing 5% fetal bovine serum (FBS, Sigma), 4 mM L-glutamine (Mediatech), 1 mM sodium pyruvate (Mediatech), 10 ng/ml epidermal growth factor (Sigma), 500 ng/ml hydrocortisone (Sigma), 5 μg/ml insulin (Sigma), 5 μg/ml transferrin (Sigma), 5 ng/ml sodium selenite (Sigma), 0.1 mM MEM non-essential amino acids (Mediatech), $10^{-4}$ M β-mercaptoethanol (Sigma), $10^3$ u/ml leukemia inhibitory factor (Millipore, Billerica, MA)) was added, cells were collected by centrifugation and $2 \times 10^4$ cells were seeded onto one gelatinized 24 well in OSE-SCM

incubation at 5% $CO_2$ for 24 hrs to eliminate accidental non-OSE cells [27,31,32]. The purity of isolated cells was confirmed by RT-PCR detection of CK8 expression.

### ALDEFLUOR assay and FACS (fluorescence activated cell sorting)

For detection of ALDH enzymatic activity primary OSE cells ($4 \times 10^6$) were placed in ALDEFLUOR buffer and processed for staining with the ALDEFLUOR Kit (Aldagen, Durham, NC) according to the manufacture's protocol. Cell sorting and data analysis were performed on a FACS Aria II sorter equipped with the FACS DiVa software (BD Bioscience, San Diego, CA). Unstained and ALDH inhibitor (4 (diethylamino)benzaldehyde [33], DEAB, at a 10-fold molar excess)-treated cells served as controls. Dead cells were excluded with propodium iodide (PI). The 5 – 8% brightest $ALDH^+$ cells were identified and electronically gated based on their characteristic light-scatter properties on the FITC channel emission pattern after excitation with 13 mW - 20 mW, 488 nm laser, elliptical shape of BD FACSAria II. The ALDH fluorescence emissions were then captured simultaneously through a 515/20 band-pass and 505 nm long-pass filter. $ALDH^+$ and $ALDH^-$ OSE cells were collected in 0.5 ml OSE-SCM and subjected to OSE-Sphere-rim-assays or RNA isolation as described below.

### OSE-sphere formation rim-assay

Cell populations ($5 \times 10^5$ cells/assay) were collected in 0.5 ml OSE-SCM, centrifuged and pellets were suspended in 1:1 reduced growth factor basement membrane matrix (Geltrex, Invitrogen, Carlsbad, CA)/OSE-SCM in a total volume of 120 µl. Following a modified protocol of Lawson et al [34] cells were placed around the rim of a well of a 12-well plate and allowed to solidify for 25 minutes at 37°C in a 5% $CO_2$ incubator before adding 1.5 ml OSE-SCM. Spheres were grown for 7 to 12 days. For passaging of spheres, media was aspirated and Geltrex was digested by incubation in 750 µl D-Buffer for 1 hr, at 37°C. During incubation spheres were suspended 2 - 3 times manually by pipetting using a blue 1 ml tip. Digested cultures were pelleted and incubated in 0.3 ml 0.25% Trypsin/EDTA for 10 min at 37°C, cells were suspended and the enzyme reaction was stopped by adding 4 ml OSE-SCM. Cells were harvested and counted by hemocytometer and cultured at different densities.

### Confocal imaging of OSE-sphere-suspension-culture

Primary OSE cells from Tgβ-actin EGFP mice at $2 \times 10^4$ cells/ml OSE Stem Cell Conditioned Medium (SCCM, DMEM/F12 (Ham's) medium (Mediatech) containing 2.4% methylcellulose (Sigma), 0.4% BSA (Sigma), 4 mM L-glutamine (Mediatech), 1 mM sodium pyruvate (Mediatech), 10 ng/ml epidermal growth factor (Sigma), 500 ng/ml hydrocortisone (Sigma), 5 µg/ml insulin (Sigma), 5 µg/ml transferrin (Sigma), 5 ng/ml sodium selenite (Sigma), 10 ng/ml fibroblast growth factor basic (Sigma), 0.1 mM MEM non-essential amino acids (Mediatech), $10^3$ u/ml leukemia inhibitory factor (Millipore), $10^{-4}$ M β-mercaptoethanol (Sigma)), were grown for 4 or 10 days in low attachment 24 wells (Corning, Corning, NY). Using a drawn-out glass capillary under a dissection microscope, spheres were washed twice for 3 minutes in a drop of PBS at room temperature (RT), fixed in 4% paraformaldehyde for 5 minutes, washed twice with PBS, once with $ddH_2O$, stained with 4′, 6-diamidiono-2-phenyindole, dilactate (DAPI, Sigma, 1 mg/ml) for 5 minutes,

transferred to a glass slide, mounted in Fluorogel (Electron Microscopy Sciences, Hatfield, PA) and covered by a glass cover slip. Confocal pictures were acquired at RT using a Zeiss LSM 510 Meta confocal microscope coupled with an Axiovert 200 inverted microscope (Carl Zeiss, Thornwood, NY). Optical sections, 512 × 512 pixels, were collected sequentially for each fluorochrome. The data sets acquired were merged and displayed with the ZEN software (Zeiss).

### Monoclonality assays

Two approaches were used. First, similarly to earlier studies in other cell types [34-36], single cell suspensions of primary OSE cells from Tgβ-actin EGFP or β-actin DsRed mice were mixed at various ratios, grown in OSE-sphere forming rim-assays for 7-12 days without sub-culture in SCCM, followed by counting the number of monochromatic and dichromatic spheres. Second, development of spheres from individual cells in rim-assays was monitored by imaging the same fields of view at different time points. All images were collected using a Nikon Eclipse TS100 microscope coupled with an Epi-Fluorescence Attachment (Nikon, Melville, NY) and equipped with a DS-L2 camera control unit and cooled camera head DS-5Mc (Nikon).

### Primary culture of the hilum and ovary parts

Individual hilum and anterior ovary parts were isolated under dissection microscope from adult virgin FVB/N mice, minced in a drop of PBS with 25G needles and transferred to 100 μl D-Buffer, following by incubation as described for the isolation of primary OSE cells. After 24 hrs adherent cultures hilum and anterior ovary part cells were collected and seeded out for the cell proliferation or OSE-sphere-rim-assays.

### Gene expression arrays

Total RNA was isolated using a mirVana miRNA isolation kit (Ambion, Austin, TX). Ovation Pico WTA System V2 (NuGen, San Carlos, CA) was used to amplify cDNA, and then labeled with biotin using Encore Biotin Module (NuGen). Labeled DNA was hybridized onto Affymetrix Mouse Genome 430 2.0 array (Affymetrix, Santa Clara, CA). All microarray analyses were performed as previously described [31,32,37,38]. Briefly, microarray data were analyzed with GeneSifter software (Geospiza, Seattle, WA). To identify genes significantly altered in ALDH positive population, we performed paired two group analysis with Significance Analysis of Microarrays (SAM) software (http://www-stat.stanford.edu/ ∼tibs/SAM) and visualized with Treeview software (http://rana.lbl.gov).

### *Trp53* and *Rb1* inactivation in primary OSE cells

Individual hilum and rest of the ovary parts were isolated under a dissection microscope from adult *Trp53*$^{loxP/loxP}$ *Rb1*$^{loxP/loxP}$ mice followed by incubation as described for the isolation of primary OSE cells. Cells were passaged one or two times and treated with recombinant adenoviruses essentially as described previously [27,31]. No changes in composition of ALDH1$^{+}$ and ALDH$^{-}$ cell subpopulations were observed during these passages, as compared to cells tested 24 hrs after initial adherent culture. At passage 6 after

*Trp53* and *Rb1* inactivation proliferation and senescence detection assays were performed as described below.

### Cell proliferation assays

Primary hilum/ovary part cells, passage 0, were harvested, reseeded in triplicates at $1 \times 10^4$ cells/3.5 cm dish in OSE-SCM, grown for three days, then stained with Giemsa solution (Sigma), air-dried and analyzed in a total area 4.92 $cm^2$. For 5-bromo-2′deoxyuridine (BrdU) staining, cells were incubated with 3 μg/ml BrdU for 2 hrs at 37°C and fixed with 4% paraformaldehyde. DNA was denatured by 4N HCl with 0.5% Triton X-100 (Sigma) at RT for 10 min, and cells were washed in Tris buffered saline with 0.5% Triton X-100. Primary antibody for BrdU (Supplementary Table 6) was applied overnight at 4°C, followed by incubation with secondary biotinylated antibody (1 hr, RT) and modified avidin-biotin-peroxidase technique was used as previously described [39].

### Senescence detection assays

For detection of senescence-associated β-galactosidase (SA-β-gal), OSE cells were fixed with 2% formaldehyde/0.2% glutaraldehyde for 5 minutes, rinsed several times with PBS, and incubated in SA-β-gal staining solution (4.2 mM citric acid, 12.5 mM sodium-phosphate, 158 mM sodium chloride, 0.21 mM magnesium chloride, 2.21 mg/ml potassium ferrocyanide, 1.68 mg/ml potassium ferricyanid (all Sigma), 1 mg/ml 5-bromo-4-chloro-3-indolyl *β*-D-galoctosidase (X-Gal, Invitrogen), pH 6.0) for 24 hrs at 37°C according to published protocol [40]. For immunofluorescent detection of p16 and p27 cells were fixed with 4% paraformaldehyde and incubated with primary antibodies (Supplementary Table 6) overnight at 4°C. Secondary antibody (Alexa Fluor 488 conjugated, Invitrogen) was applied for 1 hr at RT. DAPI was used for nuclear counterstaining.

### BrdU pulse-chase experiments

Six to 7 weeks old virgin FVB/N mice were injected daily with 250 μl of BrdU (Sigma, 1 mg/ml) intraperitoneally for 10 days (pulse) and euthanized after the pulse and at monthly intervals for 3 months in 3 independent experiments. For LCRs proliferation analysis during estrus cycle, mice were staged by vaginal cytology and sacrificed either in proestrus (prior to ovulation) or estrus (after ovulation) at 2 and 3 months of chase.

### Cell lineage tracing

To deliver the tamoxifen (Tam) pulse 6 to 7 weeks old virgin Lgr5-EGFP-IRES-creERT2 Ai9 and control mice were injected intraperitoneally with a single dose of Tam (Sigma, 0.2 mg/g body weight, 25 mg/ml in corn oil) or three times every second day for 6 days. Ovaries of Tam-pulsed mice were collected 1 and 3 days after the pulse and at monthly intervals for 2 months. Collected ovaries were fixed with 4% paraformaldehyde for 2 hours at RT, washed twice for 3 minutes with PBS, kept overnight at 4°C, embedded in Tissue-Tek O.C.T. compound (Sakura Fineted, Torrance, CA) and frozen in liquid nitrogen. Frozen sections were counterstained with DAPI (Sigma, 1 mg/ml) and images were taken with Axioskop 2 fluorescence microscope (Zeiss) equipped with a CCD camera.

### Intrabursal administration of adenovirus and carcinogenesis induction

Adult *Trp53*$^{loxP/loxP}$ / *Rb1*$^{loxP/loxP}$ mice staged at estrus, received a single trans-infundibular intrabursal injection of recombinant adenovirus AdCre-EGFP, AdCre, AdEGFP or AdBlank (Gene Transfer Vector Core, Iowa City, IA) as described previously [27]. The original stock solution (stored at -80°C) with a titer of $7 \times 10^{10}$pfu/ml was diluted 1:20 with PBS at RT immediately before the injection.

### Laser-microdissection-PCR genotyping

For microdissection of frozen sections, 5 μm thick frozen sections of the mouse ovaries were placed on slides for membrane-based laser microdissection (Leica Microsystems, Bannockburn, IL) and evaluated under the Leica DM LA microscope coupled with a Fluorescence illuminator LRF 4/22. EGFP expressing OSE from the hilum and different ovarian regions were microdissected using the Leica AS LMD laser microdissection system (Leica) equipped with a VSL-337ND-S NITROGEN laser. Phase contrast and fluorescent images were acquired before and after the microdissection. Manual microdissection of hematoxylin and eosin stained sections was performed essentially as described preciously [27,39,41]. Tissues were collected into caps of 0.6 ml centrifuge tubes filled with lysis buffer and used for subsequent PCR amplification prepared as described previously [27,37,42-44].

### Tumourigenicity assays

*Trp53 Rb1* deficient primary OSE cells derived from primary hilum or rest of the ovary were suspended in 500 μl of PBS and injected intraperitoneally ($8 \times 10^6$ cells) or subcutaneously ($5 \times 10^4$ - $5 \times 10^6$ cells) into 5 weeks old NOD.Cg-*Prkdc*$^{scid}$*Il2rg*$^{tm1Wjl}$/SzJ4 female mice. Upon signs of sickness, such as abdominal distention, intra-abdominal masses or subcutaneous masses over 1 cm in diameter, or moribund behavior mice were euthanized and subjected to necropsy.

### Morphological evaluation

Due to coiled structure of the mouse uterine tubes [45] 4 μm thick paraffin serial sections within 100 μm of the OSE/tubal epithelium junction were used for all studies of the hilum region. Serial sections were also evaluated to exclude potential misinterpretation of tangential sections in all relevant quantitative assays. All mice in carcinogenesis experiments were subjected to gross pathology evaluation during necropsy. A particular attention was paid to potential sites of ovarian carcinoma spreading, such as the omentum, regional lymph nodes, the liver, the lung and the mesentery. In addition to the ovary, pathologically altered organs, as well as representative specimens of the brain, lung, liver, kidney, spleen, pancreas, and intestine, omentum and intra-abdominal lymph nodes, were fixed in 4% PBS buffered paraformaldehyde, and evaluated by microscopic analysis of paraffin sections stained with hematoxylin and eosin, and subjected to necessary immunostainings. All early atypical lesions were diagnosed based on their morphology, staining for Ki67 and detection of floxed out *Trp53* and *Rb1* as described earlier [27]. Location of all lesions was determined by 3D reconstruction of 4 μm thick serial sections as described previously [39].

### Immunohistochemistry and quantitative image analysis

Information about all primary antibodies is provided in Supplementary Table 6. Immunohistochemical analysis of paraffin sections of paraformaldehyde-fixed tissue was performed by a modified ABC technique [37-39]. For immunofluorescence analysis, deparaffinized or frozen sections and cells were fixed in 4% paraformaldehyde. Ten-minutes treatment with 4N HCl and 10 minutes boiling in 10 mM citric buffer was used for antigen retrieval for detection of BrdU. Staining of theca cells [46] served as a positive internal control for ALDH1 detection. Sections with immunoperoxidase stainings were scanned by ScanScope (Aperio Technologies, Vista, CA) with 40X objective followed by lossless compression. Sections with immunofluorescent stainings were analyzed under an Axioskop 2 (Zeiss) fluorescence microscope equipped with a CCD camera. Quantitative analysis of IHC and IF experiments were performed with the ImageJ software (W. Rasband, National Institutes of Health, Bethesda, MD) as described previously [37-39].

### Quantitative real-time RT-PCR

All procedures were performed as described in [32] with at least 3 separately prepared RNA samples per each of 3 independent experiments. List of tested genes is indicted in Supplementary Table 3. Following primers for detection of microRNAs were obtained from Quanta Biosciences (Gaithersburg, MD): U6 small nuclear RNA, Cat. N. HSRNU6; miR-34a, Cat. N. HSMIR-0034A; miR-34b, Cat. N. MMIR-0034B-5P; miR-34c, Cat. N. HSMIR-0034C-3P; miR-376b, Cat. N. MMIR-0376B.

### Statistical analyses

All statistical analyses in this study were done using InStat 3.10 and Prism 5.04 software (GraphPad, Inc., San Diego, CA) as described previously [27,37].

## Supplementary Material

Refer to Web version on PubMed Central for supplementary material.

## Acknowledgments

We would like to thank Dr. Tudorita Tumbar for critical reading of this manuscript, Dr. Jinhyang Choi for her help with immunostainings, Dr. Lavanya Sayam (NYSTEM supported FACS Core) for her help with FACS experiments and Françoise M. Vermeylen (Cornell Statistical Consulting Unit) for her help with statistical analysis. This work was supported by grants from NIH/NCI (CA096823 and CA112354), NYSTEM (C023050 and N11G-160), and Marsha Rivkin Center for Ovarian Cancer Research to A.Y.N, NIH/NIMH (MH092928), NIH/NIA (AG040209), NYSTEM (C024323) and Russian Ministry of Education and Science to G.E. and postdoctoral fellowships to A.F.N. (NIH/NICHD T32HD052471) and C.I.H. (Cornell Comparative Cancer Biology Training Program).

## References

1. Siegel R, Naishadham D, Jemal A. Cancer statistics, 2012. CA Cancer J Clin. 2012; 62:10–29. [PubMed: 22237781]
2. Lengyel E. Ovarian cancer development and metastasis. Am J Pathol. 2010; 177:1053–1064. [PubMed: 20651229]
3. Bowtell DD. The genesis and evolution of high-grade serous ovarian cancer. Nat Rev Cancer. 2010; 10:803–808. [PubMed: 20944665]
4. Visvader JE. Cells of origin in cancer. Nature. 2011; 469:314–322. [PubMed: 21248838]

5. Auersperg N. The origin of ovarian carcinomas: a unifying hypothesis. Int J Gynecol Pathol. 2011; 30:12–21. [PubMed: 21131839]
6. Medema JP, Vermeulen L. Microenvironmental regulation of stem cells in intestinal homeostasis and cancer. Nature. 2011; 474:318–326. [PubMed: 21677748]
7. The Cancer Genome Atlas Research Network. Integrated genomic analyses of ovarian carcinoma. Nature. 2011; 474:609–615. [PubMed: 21720365]
8. Ahmed AA, et al. Driver mutations in TP53 are ubiquitous in high grade serous carcinoma of the ovary. J Pathol. 2010; 221:49–56. [PubMed: 20229506]
9. Kurman RJ, Shih Ie M. The origin and pathogenesis of epithelial ovarian cancer: a proposed unifying theory. Am J Surg Pathol. 2010; 34:433–443. [PubMed: 20154587]
10. Dubeau L. The cell of origin of ovarian epithelial tumours. Lancet Oncol. 2008; 9:1191–1197. [PubMed: 19038766]
11. Auersperg N, Woo MM, Gilks CB. The origin of ovarian carcinomas: a developmental view. Gynecol Oncol. 2008; 110:452–454. [PubMed: 18603285]
12. Seidman JD, Yemelyanova A, Zaino RJ, Kurman RJ. The fallopian tube-peritoneal junction: a potential site of carcinogenesis. Int J Gynecol Pathol. 2011; 30:4–11. [PubMed: 21131840]
13. Szotek PP, et al. Normal ovarian surface epithelial label-retaining cells exhibit stem/progenitor cell characteristics. Proc Natl Acad Sci U S A. 2008; 105:12469–12473. [PubMed: 18711140]
14. Blanpain C, Horsley V, Fuchs E. Epithelial stem cells: turning over new leaves. Cell. 2007; 128:445–458. [PubMed: 17289566]
15. Simons BD, Clevers H. Strategies for homeostatic stem cell self-renewal in adult tissues. Cell. 2011; 145:851–862. [PubMed: 21663791]
16. Ginestier C, et al. ALDH1 is a marker of normal and malignant human mammary stem cells and a predictor of poor clinical outcome. Cell Stem Cell. 2007; 1:555–567. [PubMed: 18371393]
17. Storms RW, et al. Isolation of primitive human hematopoietic progenitors on the basis of aldehyde dehydrogenase activity. Proc Natl Acad Sci U S A. 1999; 96:9118–9123. [PubMed: 10430905]
18. Corti S, et al. Identification of a primitive brain-derived neural stem cell population based on aldehyde dehydrogenase activity. Stem Cells. 2006; 24:975–985. [PubMed: 16293577]
19. Burger PE, et al. High aldehyde dehydrogenase activity: a novel functional marker of murine prostate stem/progenitor cells. Stem Cells. 2009; 27:2220–2228. [PubMed: 19544409]
20. Deng S, et al. Distinct expression levels and patterns of stem cell marker, aldehyde dehydrogenase isoform 1 (ALDH1), in human epithelial cancers. PLoS One. 2010; 5:e10277. [PubMed: 20422001]
21. Bullough WS. Oogenesis and its relation to the oestrous cycle in the adult mouse. Journal of Endocrinology. 1942; 3:141–149.
22. Ji Q, et al. MicroRNA miR-34 inhibits human pancreatic cancer tumor-initiating cells. PLoS One. 2009; 4:e6816. [PubMed: 19714243]
23. Liu C, et al. The microRNA miR-34a inhibits prostate cancer stem cells and metastasis by directly repressing CD44. Nat Med. 2011; 17:211–215. [PubMed: 21240262]
24. Choi YJ, et al. miR-34 miRNAs provide a barrier for somatic cell reprogramming. Nat Cell Biol. 2011; 13:1353–1360. [PubMed: 22020437]
25. Barker N, et al. Identification of stem cells in small intestine and colon by marker gene Lgr5. Nature. 2007; 449:1003–1007. [PubMed: 17934449]
26. Madisen L, et al. A robust and high-throughput Cre reporting and characterization system for the whole mouse brain. Nat Neurosci. 2010; 13:133–140. [PubMed: 20023653]
27. Flesken-Nikitin A, Choi KC, Eng JP, Shmidt EN, Nikitin AY. Induction of carcinogenesis by concurrent inactivation of p53 and Rb1 in the mouse ovarian surface epithelium. Cancer Res. 2003; 63:3459–3463. [PubMed: 12839925]
28. Szabova L, et al. Perturbation of Rb, p53, and Brca1 or Brca2 Cooperate in Inducing Metastatic Serous Epithelial Ovarian Cancer. Cancer Res. 2012; 72:4141–4153. [PubMed: 22617326]
29. Pellegrini G, et al. Location and clonal analysis of stem cells and their differentiated progeny in the human ocular surface. J Cell Biol. 1999; 145:769–782. [PubMed: 10330405]

30. Barker N, et al. Lgr5(+ve) stem cells drive self-renewal in the stomach and build long-lived gastric units in vitro. Cell Stem Cell. 2010; 6:25–36. [PubMed: 20085740]
31. Corney DC, Flesken-Nikitin A, Godwin AK, Wang W, Nikitin AY. MicroRNA-34b and MicroRNA-34c are targets of p53 and cooperate in control of cell proliferation and adhesion-independent growth. Cancer Res. 2007; 67:8433–8438. [PubMed: 17823410]
32. Hwang CI, et al. Wild-type p53 controls cell motility and invasion by dual regulation of MET expression. Proc Natl Acad Sci U S A. 2011; 108:14240–14245. [PubMed: 21831840]
33. Russo JE, Hauguitz D, Hilton J. Inhibition of mouse cytosolic aldehyde dehydrogenase by 4-(diethylamino)benzaldehyde. Biochem Pharmacol. 1988; 37:1639–1642. [PubMed: 3358794]
34. Lawson DA, Xin L, Lukacs RU, Cheng D, Witte ON. Isolation and functional characterization of murine prostate stem cells. Proc Natl Acad Sci U S A. 2007; 104:181–186. [PubMed: 17185413]
35. Xin L, Lukacs RU, Lawson DA, Cheng D, Witte ON. Self-renewal and multilineage differentiation in vitro from murine prostate stem cells. Stem Cells. 2007; 25:2760–2769. [PubMed: 17641240]
36. Singec I, et al. Defining the actual sensitivity and specificity of the neurosphere assay in stem cell biology. Nat Methods. 2006; 3:801–806. [PubMed: 16990812]
37. Zhou Z, et al. Synergy of p53 and Rb deficiency in a conditional mouse model for metastatic prostate cancer. Cancer Res. 2006; 66:7889–7898. [PubMed: 16912162]
38. Choi J, Curtis SJ, Roy DM, Flesken-Nikitin A, Nikitin AY. Local mesenchymal stem/progenitor cells are a preferential target for initiation of adult soft tissue sarcomas associated with p53 and Rb deficiency. Am J Pathol. 2010; 177:2645–2658. [PubMed: 20864684]
39. Nikitin A, Lee WH. Early loss of the retinoblastoma gene is associated with impaired growth inhibitory innervation during melanotroph carcinogenesis in Rb+/- mice. Genes Dev. 1996; 10:1870–1879. [PubMed: 8756345]
40. Debacq-Chainiaux F, Erusalimsky JD, Campisi J, Toussaint O. Protocols to detect senescence-associated beta-galactosidase (SA-betagal) activity, a biomarker of senescent cells in culture and in vivo. Nat Protoc. 2009; 4:1798–1806. [PubMed: 20010931]
41. Matoso A, Zhou Z, Hayama R, Flesken-Nikitin A, Nikitin AY. Cell lineage-specific interactions between Men1 and Rb in neuroendocrine neoplasia. Carcinogenesis. 2008; 29:620–628. [PubMed: 17893233]
42. Nikitin AY, Lee WH. Early loss of the retinoblastoma gene is associated with impaired growth inhibitory innervation during melanotroph carcinogenesis in *Rb*$^{+/-}$ mice. Genes & Development. 1996; 10:1870–1879. [PubMed: 8756345]
43. Zhou Z, Flesken-Nikitin A, Nikitin AY. Prostate cancer associated with p53 and Rb deficiency arises from the stem/progenitor cell-enriched proximal region of prostatic ducts. Cancer Res. 2007; 67:5683–5690. [PubMed: 17553900]
44. Zhou Z, et al. Suppression of melanotroph carcinogenesis leads to accelerated progression of pituitary anterior lobe tumors and medullary thyroid carcinomas in Rb+/- mice. Cancer Res. 2005; 65:787–796. [PubMed: 15705875]
45. Rugh, R. The Mouse Its Reproduction and Development. Oxford University Press; Oxford: 1990.
46. Vermot J, Fraulob V, Dolle P, Niederreither K. Expression of enzymes synthesizing (aldehyde dehydrogenase 1 and reinaldehyde dehydrogenase 2) and metabolizaing (Cyp26) retinoic acid in the mouse female reproductive system. Endocrinology. 2000; 141:3638–3645. [PubMed: 11014218]

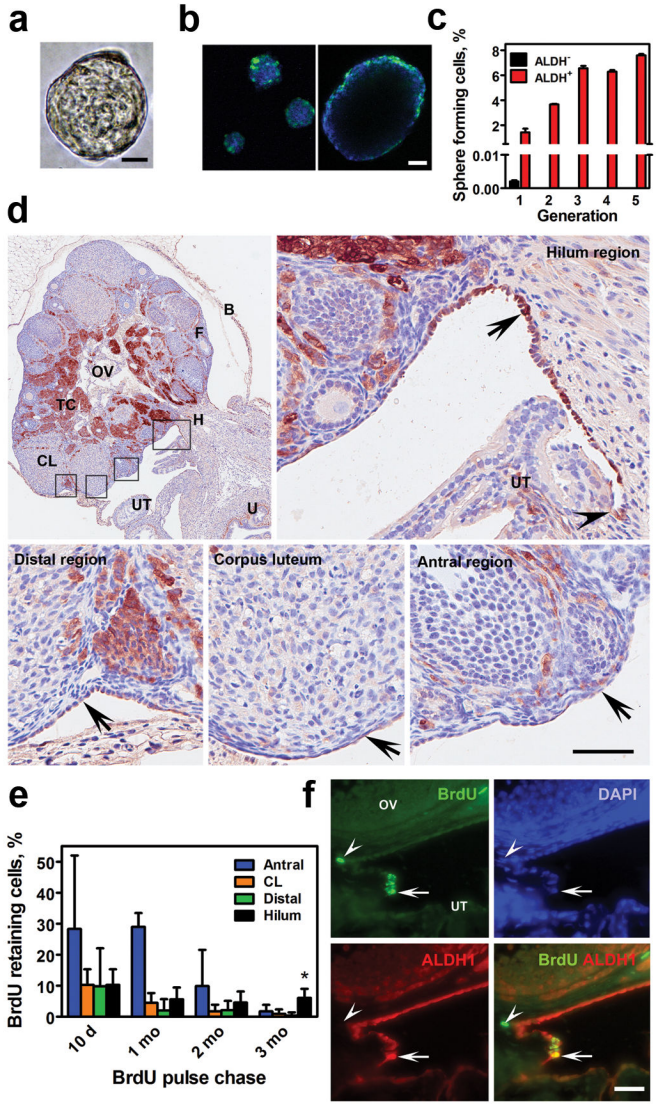


**Figure 1. Identification and location of putative OSE stem cells**

**a**, OSE sphere, Phase contrast. Bar, 20 μm. **b**, Confocal imaging of compact (left) and expanded (right) OSE spheres from Tgβ-actin EGFP mice at 4 and 10 days, respectively. Green fluorescence, counterstaining with DAPI, blue. Bar, both images, 50 μm. **c**, Frequency of sphere formation by ALDH$^-$ and ALDH$^+$ OSE cells for 5 consecutive generations (G, dissociation/clonal formation; $n = 6$, mean ± s.d.). ALDH$^-$ derived cells very rarely formed spheres in G2 and did not yield any spheres in G3. **d**, ALDH1 (brown color) is preferentially expressed in the OSE (arrows) of the hilum region as compared to that of the antral region, corpus luteum or distal region. ALDH1 staining is also present in the theca cells (TC) of the ovary. Rectangles in top left image indicate respective location (clockwise) of the regions in the mouse ovary. Arrowhead, the junction between OSE and tubal epithelium. B, bursa; CL, corpus luteum; F, follicle; H, hilum; OV, ovary; TC, theca cells; UT, uterine tube; U, uterus. 6 weeks old mouse. ABC Elite method, hematoxylin counterstaining. Bar, top left image, 500 μm; all other images, 50 μm. **e**, Quantification of

BrdU label retaining cells (LRCs) in the antral, corpus luteum (CL), distal and hilum regions ($n$ = 4, mean ± s.d.). At 3 months after BrdU pulse two tailed $P$: hilum (*) versus antral region, 0.0005; versus CL or distal region, < 0.0001. **f**, Detection of BrdU LRCs (green), ALDH1 (red) and overlay (orange) in the hilum OSE (arrows) after 3 months of chase. Arrowhead, BrdU LRC in the neighboring stroma. Counterstaining with DAPI, blue. Bar, 50 μm.

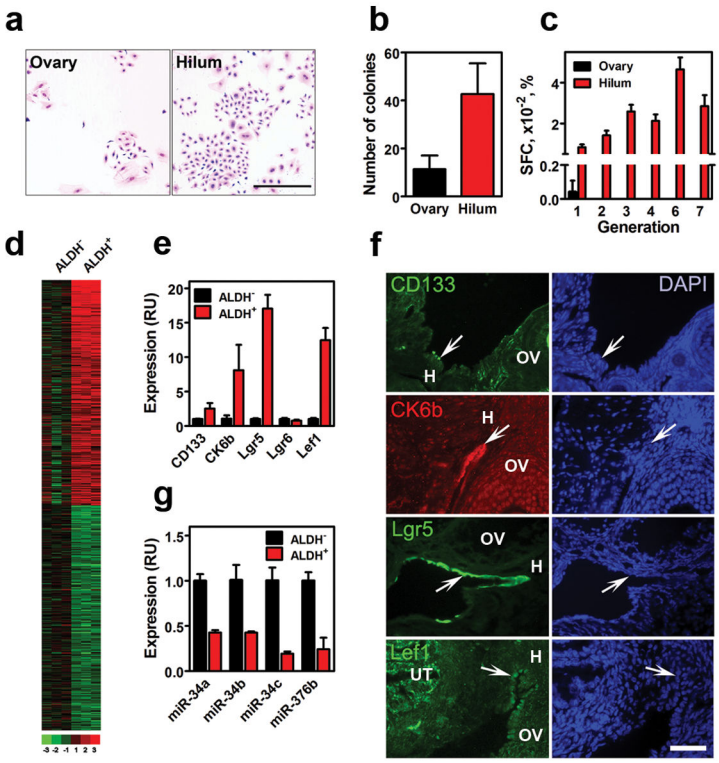


**Figure 2. Functional characterization of the hilum OSE cells**

**a**, Colony formation by OSE cells isolated from the anterior part (Ovary) and the hilum. 4.0 × $10^3$ cells per plate. Giemsa staining. Bar, 500 μm. **b**, Quantitative analysis of frequency of large colonies (≥ 20 cells) formed by OSE cells from the anterior part (*n* = 8, mean ± s.d., 11.4 ± 5.68) and the hilum (*n* = 6, 42.7 ± 12.8). Two tailed *P* < 0.0001. **c**, Frequency of the anterior part and hilum OSE sphere forming cells (SFC) for 1 (Ovary) 1 and 7 (hilum) consecutive generations (G, *n* = 3, mean ± s.d.). Anterior part derived cells very rarely formed spheres in G2 and did not yield any spheres in G3. **d**, Gene expression profiles of 3 independent pools (10 mice each) of $ALDH^-$ and $ALDH^+$ cells. **e**, Expression of stem cell markers in $ALDH^-$ and $ALDH^+$ cells. Quantitative PCR (*n* =3, mean ± s.d.; all *P* values <0.01, except for Lgr6). **f**, Detection of hilum cells (arrows) expressing CD133, CK6b, Lgr5 and Lef1. Immunofluorescence (CD133, CK6b, and Lef1) or EGFP expression under the control of *Lgr5* promoter in Lgr5-EGFP-IRES-creERT2 mouse. All abbreviations as in Fig. 1d. Counterstaining with DAPI, blue. Bar for all images, 50 μm. **g**, Expression of microRNAs in $ALDH^-$ and $ALDH^+$ cells. Quantitative PCR (*n* = 3, mean ± s.d.; all *P* values <0.01).

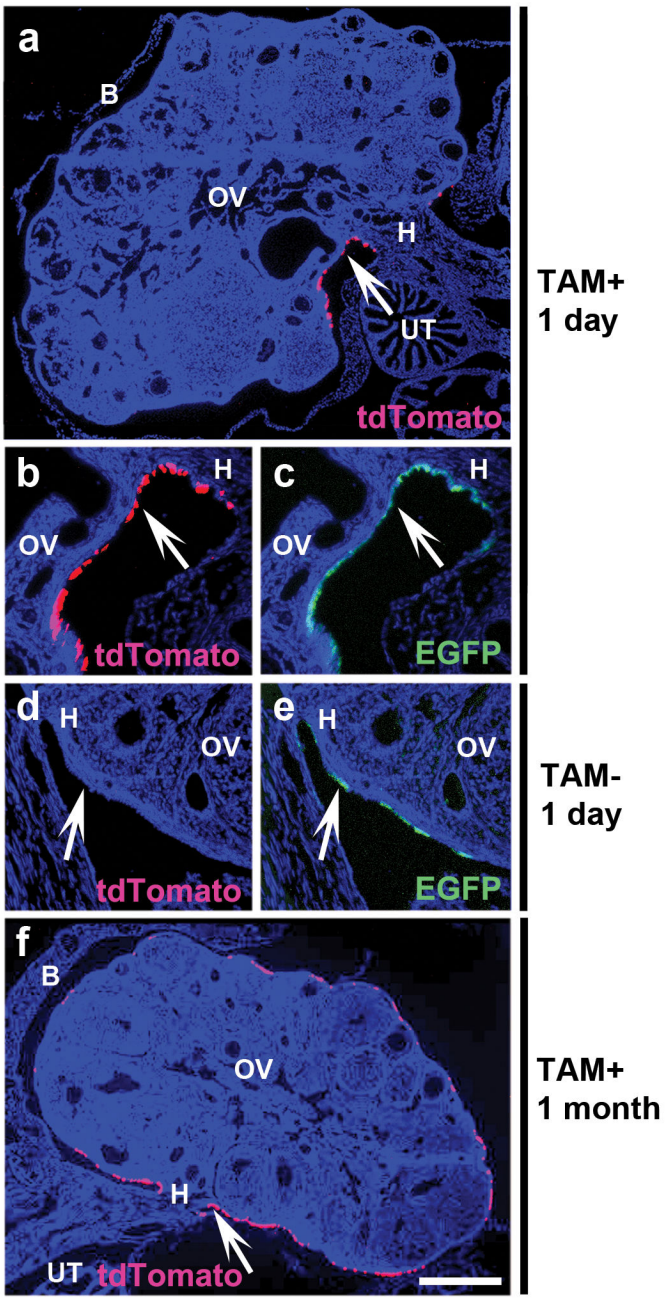


**Figure 3. Tracing the fate of the Lgr5$^{+}$ hilum cells**

**a-f**, Detection of tdTomato (red, a, b, d, f) and EGFP (green, c, e) expression in the ovaries of Lgr5-EGFP-IRES-creERT2 Ai9 mice 1 day (a-e) and 1 month (f) after administration of either tamoxifen (a-c, f) or vehicle (d, e). All abbreviations as in Fig. 1d. Counterstaining with DAPI, blue. Arrows, hilum OSE. Bar, a, f, 600 μm; b-e, 130 μm.

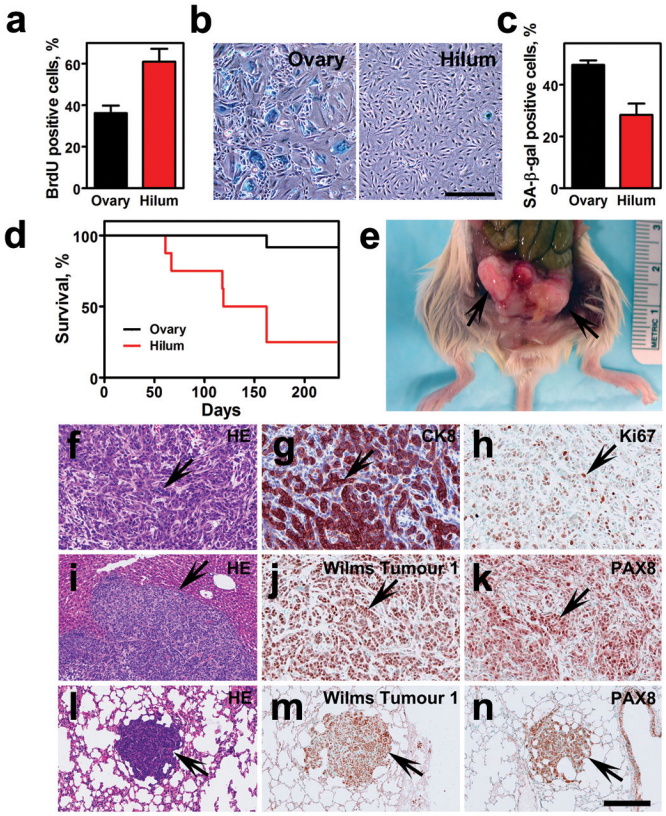


**Figure 4. Hilum cells show preferential transformation after conditional inactivation of *Trp53* and *Rb1***

**a-c**, Characterization of primary OSE cells isolated from the hilum and the remainder of the ovary (Ovary) and evaluated at passage 6 after Cre-*loxP* mediated inactivation of *Trp53* and *Rb1*. Quantification of BrdU positive OSE cells (a, $n = 3$, mean ± s.d., $P < 0.0001$). Detection (b) and quantitative analysis (c) of senescence associated-β-galactosidase (blue) in the ovary and hilum cells (c, $n = 3$, mean ± s.d., two tailed $P = 0.002$). Phase contrast. Bar, 500 μm. **d**, Survival of mice intraperitoneally transplanted with primary ovary ($n = 12$) and hilum ($n = 8$) OSE cells deficient for *Trp53* and *Rb1* (log-rank $P = 0.0007$). **e**, Neoplastic masses (arrows) arisen from hilum cells transplanted into the mouse abdominal cavity. **f-n**, Hilum derived-neoplastic cells have marked nuclear atypia (f), express cytokeratin 8 (CK8, g), are highly proliferative (h), grow in solid, nested and gland-like patterns (f-h, j, k, arrows), invade liver (i, arrow), metastasize to the lung (l-n, arrows) and express Wilms Tumour 1 (j, m) and PAX8 (k, n). Hematoxylin and eosin (HE) and immunostainings, ABC Elite method. Counterstaining with hematoxylin (CK8) and methyl green (Ki67, Wilms Tumour 1, PAX8). Bar, f-h, j, k, 100 μm; i, l-n, 200 μm.